NGVLA Memo 68: Imaging the Dusty Substructures due to Terrestrial Planets in Planet-forming Disks with the Next Generation Very Large Array

S. K. Harter[1], L. Ricci[1,*], S. Zhang[2], Z. Zhu[2]

[1] *Department of Physics and Astronomy, California State University Northridge, 18111 Nordhoff Street, Northridge, CA 91330, USA*

[2] *Department of Physics and Astronomy, University of Nevada Las Vegas, Las Vagas, NV 89154, USA*

[*] *Corresponding author: Luca Ricci, luca.ricci@csun.edu*

Abstract. We present simulations of the capabilities of the Next Generation Very Large Array to detect and resolve substructures due to planets in the dust emission of nearby planet-forming disks. The main goal of this study is to determine the masses and orbital radii of planets which can leave signatures in the disk dust continuum emission that an instrument like the ngVLA, with its current design, would be capable to detect. Whereas previous studies on the disk-planet interaction focused on planets with masses of about 10 $M_{\rm Earth}$ and larger, this study investigates the effects of lower mass planets down to Earth-mass planets around Solar-mass young stars and Mars-mass planets around young M-type stars. For this investigation we adopt the results of global 2-D hydrodynamical planet-disk simulations that account for the dynamics of gas and dust in a disk with an embedded planet. Our work shows that the ngVLA can detect and spatially resolve dust structures due to low-mass rocky planets in the terrestrial planet formation regions of nearby disks, under the assumption that the disk viscosity in those regions is low.

1. Introduction

The mutual interaction between planets and the parental disk plays a prominent role in setting the main physical properties of planets. Planets are made of solids and gas which come from the disk, and the gravitational interaction between a newly born planet and the material in the disk can strongly affect the history of its location within the planetary system (for a review see Baruteau et al. 2014).

Recent hi-res observations at both optical/near-infrared and sub-millimeter/millimeter wavelengths have shown that structures in disks which resemble the predictions from planet-disk interaction theory are ubiquitous in young nearby disks (e.g., Benisty et al. 2015, Dipierro et al. 2018, Andrews et al. 2018). The detailed modeling of the observed disk substructures, especially rings and gaps, are now routinely being used to infer key properties of the putative young planets, such as mass and orbital radius. These studies show that the rings and gaps seen by ALMA from observations of the disk dust continuum likely trace a population of relatively massive young planets, with

masses $\gtrsim$ 10 $M_\oplus$, and relatively far from the host stars, at orbital distances $\gtrsim$ 10 au (Zhang et al. 2018, Long et al. 2018, Lodato et al. 2019).

Owing to different observational biases, the populations of these young planets and of the detected mature exoplanets have a very scarce overlap on the popular (planet mass, orbital radius) plane. This strongly hinders comparison investigations between the properties of these young vs mature exoplanet populations which are key to unveil the processes of formation and early evolution of planetary systems (see discussion in Lodato et al. 2019). Future improvements on the observational capabilities regarding both direct and indirect methods of exoplanet detection will be necessary to inform theories of planet formation and evolution.

Given the expected angular resolution ($\approx$ milliarcsec) and sensitivity at long wavelengths ($\gtrsim$ 3mm), a future Next Generation Very Large Array (ngVLA, Murphy et al. 2018) would be able to spatially resolve structures in the disk dust continuum within the inner disk regions of terrestrial planet formation (1 au at the distance of the closest star forming regions, i.e. 140 pc, corresponds to an angular scale of about 7 milliarcsec). In this study we aim to quantify the capabilities of the ngVLA to detect and spatially resolve disk structures due to the interaction with planets with masses $\lesssim$ 10 $M_\oplus$ at orbital separations $\lesssim$ 5 au from the host star, which are more in line with the properties of the bulk of the population of mature exoplanets detected so far.

Ricci et al. (2018) already tested the capabilities of the ngVLA to image disk substructures due to planets in the dust continuum emission of nearby disks. However, the simulations that were run for that study followed the evolution of their disk-planet systems for up to 2000 planetary orbits. The models presented here follow the disk evolution for more orbits, giving more time for low-mass terrestrial planets to open gaps in the dust density of low-viscosity disks that can be detected by the ngVLA (see, e.g., Dong et al. 2018).

Section 2 presents the methods used for this study, describing the disk physical models used to simulate the disk-planet interaction, the procedure used to obtain the model synthetic images at the ngVLA and ALMA wavelengths, and the method used to simulate the results of future ngVLA and ALMA observations. Section 3 outlines the results of this investigation, whereas Section 4 presents the conclusion of this work.

2. Methods: from disk simulations to ngVLA and ALMA observations

We describe here the method used to simulate observations with the ngVLA and ALMA for the dust continuum emission of disks with embedded low-mass terrestrial planets.

2.1. Disk model

The models used for this investigation were obtained via 2D hydrodynamical planet–disk simulations using the modified version of the grid-based code FARGO (Masset 2000) called Dusty FARGO-ADSG (Baruteau & Masset 2008a, 2008b; Baruteau & Zhu 2016). This code accounts for the dynamics of gas and dust in a disk with one or more embedded planets. In particular, it can calculate the gravitational interaction between gas and dust with the planet as well as the aerodynamical gas-drag on the dust.

We refer to Zhang et al. (2018) for a detailed description of the physical structure of the disk models and method to extract synthetic images for the dust continuum at different wavelengths for a given model. In the models discussed here we considered

disks with a dust grain size distribution $n(s) \propto s^{-3.5}$ with maximum grain size of 1 cm, a disk aspect ratio at the orbital radius r_p of the planet $h/r\ (r_p) = 0.03$, a viscosity parameter $\alpha = 10^{-5}$ constant across the disk, an initial gas surface density at the planet location $\Sigma_{\rm gas}(r_p) = 300$ g/cm^2, and stellar luminosity $L_\star = 1, 5, 10\ L_\odot$.

In these models, the planet mass enters in the ratio q with the stellar mass. We investigated models with $q = M_p/M_\star = 1\ M_\oplus/M_\odot$ and $10\ M_\oplus/M_\odot$, corresponding to an Earth-mass planet and 10 $M_\oplus$-mass Super Earth around a solar-mass star, or a Mars-mass planet and Earth-mass planet around a 0.1 $M_\odot$ M-type young star, respectively. Each simulation was run for up to 7000 planet orbits with the planet at 1, 2 or 3 au from the host star. The synthetic maps for the dust continuum emission of the models were derived at wavelengths of 1.25mm, 3mm, 7mm and 1cm, and two representative cases are shown in Figure 1.

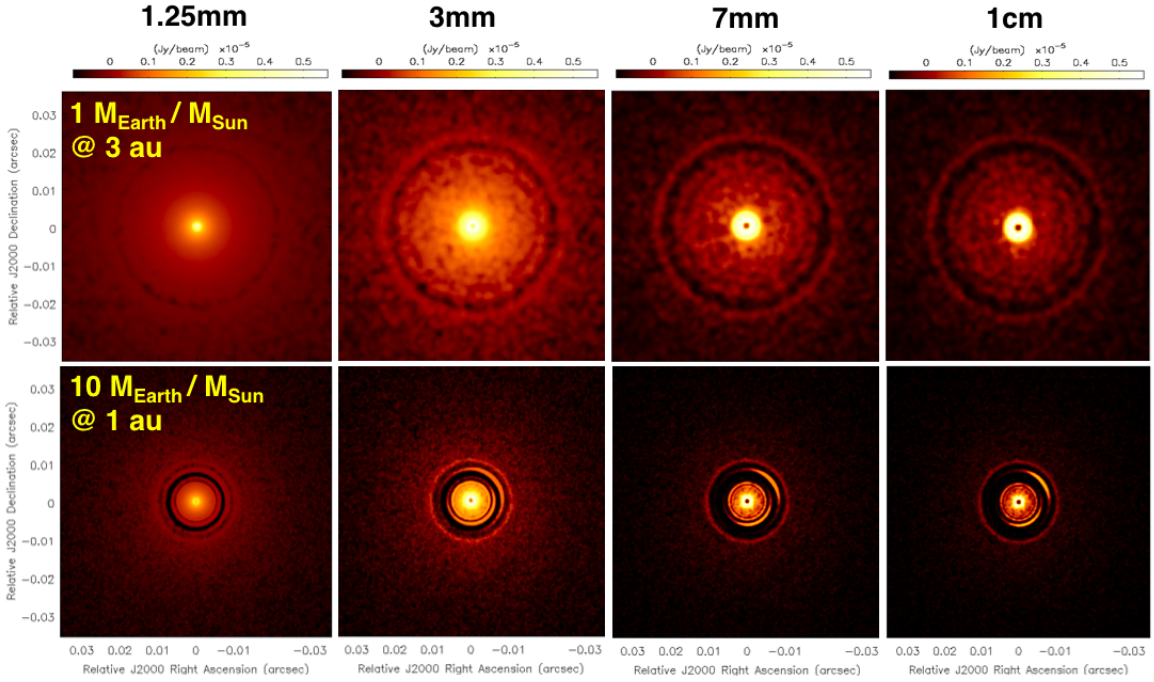

Figure 1. Model synthetic images for the dust continuum emission at 1.25, 3, 7 and 10 mm for two of the systems considered in this study. Top row) Disk model with a planet at 3 au from the host star and a planet-star mass ratio of 1 $M_\oplus/M_\odot$. The integrated flux densities for the models are 42.0, 4.2, 0.32 and 0.099 mJy at the wavelengths of 1.25, 3, 7 and 10 mm, respectively. Bottom row) Disk model with a planet at 1 au from the host star and a planet-star mass ratio of 10 $M_\oplus/M_\odot$. The integrated flux densities for the models are 15.0, 1.4, 0.099 and 0.031 mJy at the wavelengths of 1.25, 3, 7 and 10 mm, respectively.

2.2. Simulations of the ngVLA and ALMA observations

The synthetic maps obtained according to the method outlined in Section 2.1 were converted into predictions for future observations with the ngVLA (at $\lambda = 3, 7, 10$mm) and ALMA ($\lambda = 1.25$mm) using the CASA software package (McMullin et al. 2007). We adopted the same procedure as in Ricci et al. (2018), in which the ngVLA simulations

are performed using the `SIMOBSERVE` task to generate the visibility dataset in the (u, v) Fourier space, and the `SIMNOISE` task to add the noise by corrupting the visibilities.

For the ngVLA simulations we considered the original ngVLA Rev B array configuration distributed across the US Southwest and Mexico. The Rev B configuration includes 214 antennas of 18 meter diameter, to baselines up to 1000 km (Selina et al. 2018). We instead did not include the 30 additional antennas distributed to baselines up to 9000 km, as the signal from the sources considered here would be very faint for these very long baselines. For the array configuration of the ALMA observations, we used the `alma.out28.cfg` antenna position file available in the CASA package, which contains the longest 16 km baselines in the ALMA array.

For the imaging of the visibilities we employed the `CLEAN` algorithm with Briggs weighting, and adjusted the robust parameter to give a reasonable synthesized beam and noise performance. In particular, the ALMA images were computed with a Briggs weighting with robust parameter $R = -2$ (uniform weighting), while for the ngVLA we chose $R = -1$. We also employed a multiscale clean approach to better recover compact emission at both high brightness and large diffuse structures in the model. The disk center was located at a declination of +24.0 degrees for the ngVLA simulations and −24.0 degrees for the ALMA simulations, and the assumed distance is 140pc.

3. Results

Figure 2 shows the results of the ngVLA and ALMA simulations for the disk model with a planet at 3 au from the central star and planet-star mass ratio of 1 $M_\oplus/M_\odot$ at wavelengths of 1.25, 3, 7 and 10 mm, respectively.

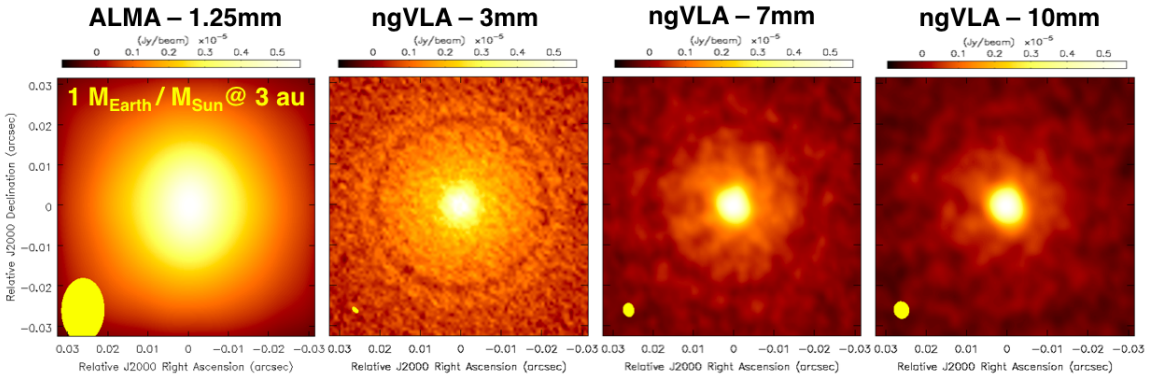

Figure 2. ALMA and ngVLA simulated observations for the dust continuum emission at 1.25, 3, 7 and 10 mm for the disk model with a planet at 3 au and planet-star mass ratio of 1 $M_\oplus/M_\odot$. In the bottom left corner of each panel the yellow ellipse shows the synthesized beam, and has sizes of 18mas×12mas, 1.9mas×1.0mas, 3.4mas×2.7mas and 4.2mas×3.7mas at 1.25, 3, 7 and 10 mm, respectively. The rms noise on each map is 2800, 86, 35 and 21 nJy/beam at 1.25, 3, 7 and 10 mm, respectively.

As shown in the figure, the ngVLA provides enough resolution to probe the innermost disk regions of terrestrial planet formation. At the distance of 140pc, the spatial resolution of the ngVLA corresponds to 0.27au × 0.14au at 3mm and 0.59au × 0.52au at 10 mm, respectively. The rms noise levels for the ngVLA simulations correspond to

integration times of about 100 hours according to the current ngVLA reference design (Table 7 in Selina et al. 2018).

The impact of the rms noise on the observability of gaps/rings induced by low-mass planets with orbital radii of 2 and 3 au are investigated in Figure 3. This figure shows that these gaps should be observable at 3mm already after $\sim$ 20 hours of integration time (rms noise $\approx$ 170 nJy beam^{-1}).

Figures 4 and 5 present the ngVLA and ALMA simulations for the disk model with planets with planet-star mass ratio of 10 $M_\oplus/M_\odot$ (10 $M_\oplus$ super-Earth around a Solar-mass young star or Earth-mass planet around a 0.1 $M_\odot$ M-type young star) at 3 and 1 au from the central star, respectively.

Figure 4 shows that, whereas ALMA at 1.25mm can detect a decrease in the continuum surface brightness along the orbit of the planet, the ngVLA can resolve the gap at 3, 7 and 10 mm, and can also detect azimuthal structures that are expected by planet-disk interaction in disks with low viscosity. Moreover, the dependence of these structures with wavelength (e.g., their radial and azimuthal extent) can be used to investigate the optical depth of the dust emission, the properties of the emitting dust grains and of the aerodynamical interaction with the underlying gas (e.g., Casassus et al. 2019), and would allow us to further explore the physics of planet-disk interaction. Figure 5 shows that the ngVLA would detect a decrease in the continuum surface brightness at 3mm induced by a planet at 1 au even after an integration time of $\approx$ 6 hours.

4. Conclusions

The ngVLA will transform the fields of planet formation and protoplanetary disks, allowing for imaging of the disk physical structure at sub-au resolution in nearby star forming regions.

In this study we tested the imaging capabilities of the ngVLA, and the comparison with ALMA, for resolving gaps and rings and other substructures in the dust continuum of disks with low viscosity due to low-mass terrestrial planets around Solar-mass and 0.1 $M_\odot$ M-type young stars.

We showed that in these systems terrestrial planets with orbital radii of $1-3$ au can leave imprints in the dust continuum emission that the ngVLA would be able to detect in $\sim$ 5 – 10 hours of integration time. Deeper observations with longer integration ($>$ 20 hours) would then allow us to well characterize the radial structure of the main rings/gaps, and also detect emission from azimuthal structures close to the planet as expected by physical models of the planet-disk interaction in disks with low viscosity.

Furthermore, multi-wavelength observations within the range of frequencies covered by the ngVLA would allow us to map the spectral index in regions of local dust concentration. This is necessary to constrain observationally the spatial segregation of grains with different sizes, better quantify the dust optical depth at these wavelengths and further constrain the physical process of planet-disk interaction.

This work presents the results of a relatively narrow region of the space of the relevant disk parameters (e.g., disk density, gas viscosity). Further details on the models as well as the predictions for future ngVLA and ALMA observations over a broader region of the parameter space of the models will be provided in a future paper (Harter et al. in prep.).

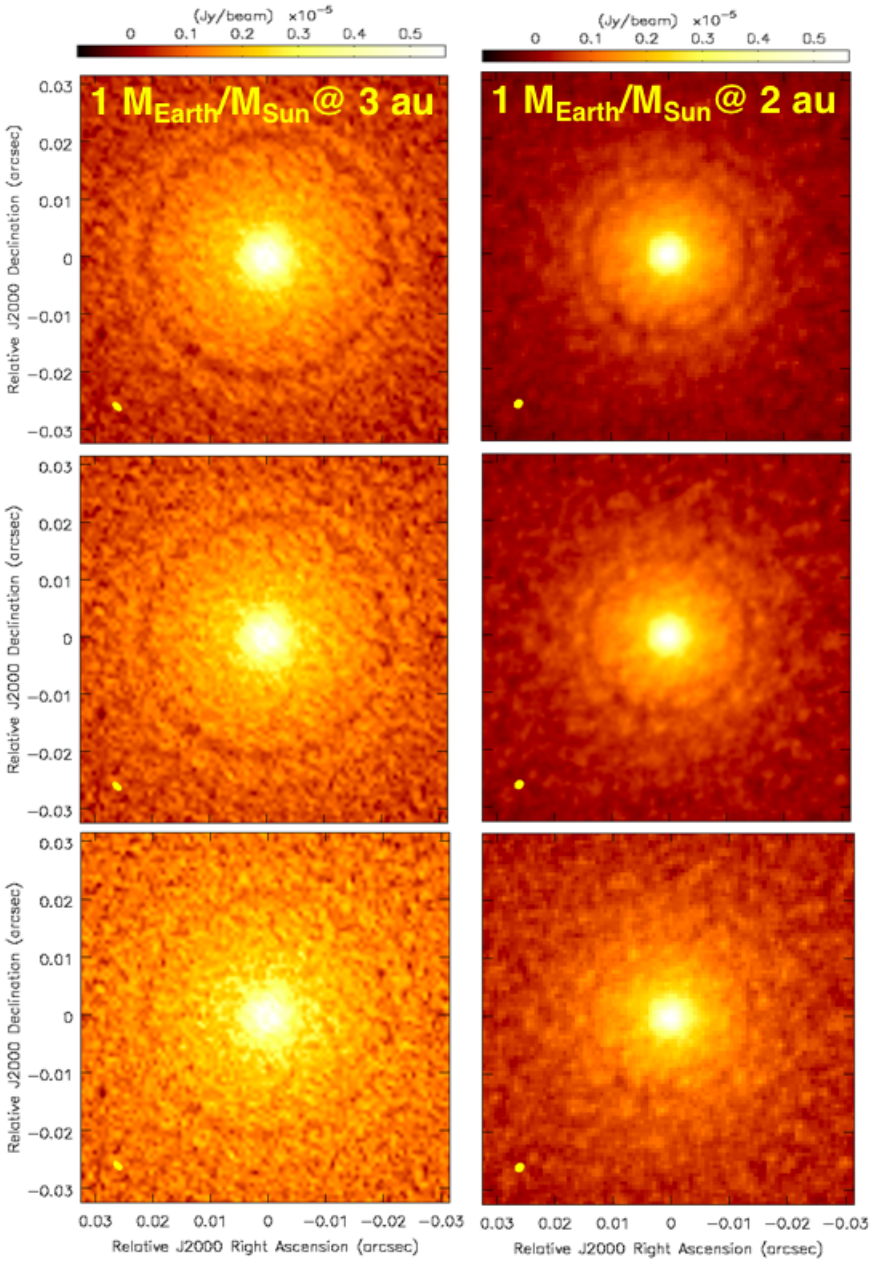

Figure 3. ngVLA simulated observations for the dust continuum emission at 3 mm for disk models with a planet with planet-mass ratio of 1 $M_{\oplus}/M_{\odot}$ at 3 au (left column) and 2 au (right) from the host star. Left column) In each panel the synthesized beam has sizes of 1.9mas × 1.0mas, and the rms noise is 86, 114 and 177 nJy/beam from top to bottom, respectively. Right column) In each panel the synthesized beam has sizes of 1.7mas × 1.3mas, and the rms noise is 86, 115 and 172 nJy/beam from top to bottom, respectively.

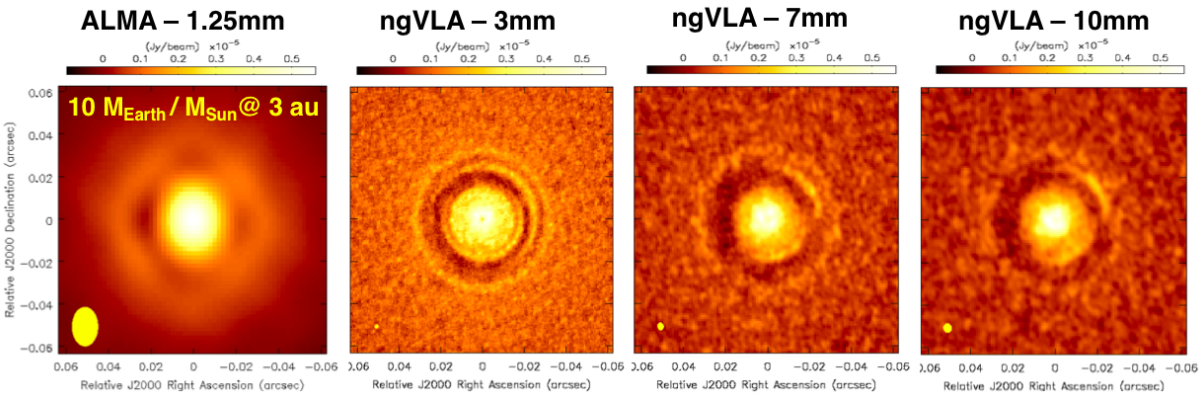

Figure 4. ALMA and ngVLA simulated observations for the dust continuum emission at 1.25, 3, 7 and 10 mm for the disk model with a planet at 3 au and planet-star mass ratio of 10 $M_\oplus/M_\odot$. In the bottom left corner of each panel the yellow ellipse shows the synthesized beam, and has sizes of 18mas×12mas, 1.7mas×1.3mas, 3.4mas×2.7mas and 4.2mas×3.7mas at 1.25, 3, 7 and 10 mm, respectively. The rms noise on each map is 2800, 86, 35 and 21 nJy/beam at 1.25, 3, 7 and 10 mm, respectively.

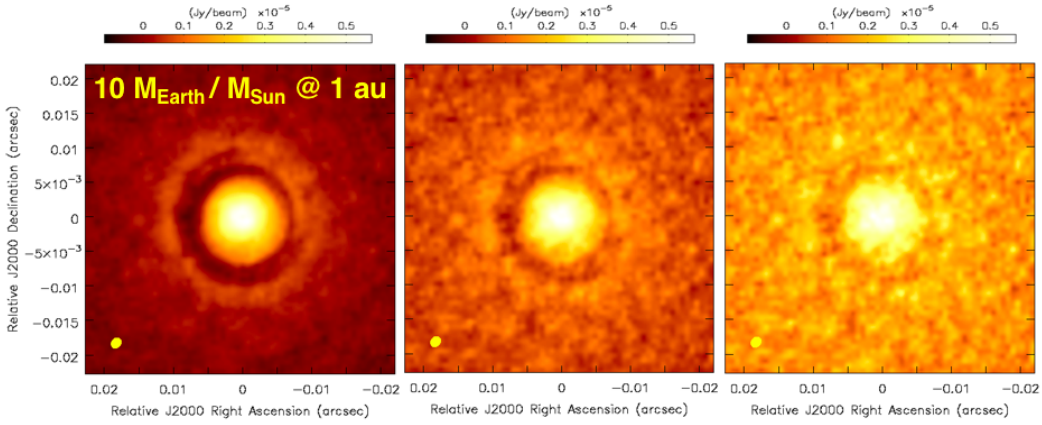

Figure 5. ngVLA simulated observations for the dust continuum emission at 3mm for the disk model with a planet at 1 au and planet-star mass ratio of 10 $M_\oplus/M_\odot$. In each panel the synthesized beam has sizes of 1.7mas × 1.3mas. The rms noise on each map is 86, 172 and 343 nJy/beam from left to right, respectively.

Acknowledgments. This work was supported in part by the ngVLA Community Studies program, coordinated by the National Radio Astronomy Observatory, which is a facility of the National Science Foundation operated under cooperative agreement by Associated Universities, Inc.

References

Andrews, S., Huang, J., Perez, L., et al. 2018, ApJ 869, 41

Baruteau, C., & Zhu, Z. 2016, MNRAS 458, 3927
Baruteau, C., Crida, A., Paardekooper, S.-J., et al. 2014, in Protostars and Planets VI, ed. H. Beuther et al. (Tucson, AZ: Univ. Arizona Press), 667
Baruteau, C., & Masset, F. 2008a, ApJ 672, 1054
Baruteau, C., & Masset, F. 2008b, ApJ 678, 483
Benisty, M., Juhasz, A., Boccaletti, A., et al. 2015, A&A 578, 6
Carilli, C. 2018, ngVLA Memo No. 47
Casassus, S., Marino, S., Lyra, W., et al. 2019, MNRAS 483, 3278
Dipierro, G., Ricci, L., Perez, L., Lodato, G. et al. 2018, MNRAS 475, 5296
Dong, R., Li, S., & Chiang, E. 2018, ApJ 866, 110
Lodato, G., Dipierro, G., Ragusa, E., et al. 2019, MNRAS 486, 453
Long, F., Pinilla, P., Herczeg, G., et al., 2018, ApJ 869, 17
Masset, F. 2000, A&AS 141, 165
McMullin, J. P., Waters, B., Schiebel, D., Young, W., & Golap, K. 2007, in ASP Conf. Ser. 376, Astronomical Data Analysis Software and Systems XVI (San Francisco, CA: ASP), 127
Murphy, E. J., Bolatto, A., Chatterjee, S. et al. 2018, Science with a Next Generation Very Large Array, ASP Conference Series, Vol. 517. ASP Monograph 7. Edited by Eric Murphy., p.3
Ricci, L., Liu, S.-F., Isella, Andrea; Li, H. 2018, ApJ 853, 110
Selina, R. J., Murphy, E. J., McKinnon, M., Beasley, A., Butler, B., Carilli, C. et al. 2018, Science with a Next Generation Very Large Array, ASP Conference Series, Vol. 517. ASP Monograph 7. Edited by Eric Murphy., p.15
Zhang, S., Zhu, Z., Huang, J., Guzman, V. et al. 2018, ApJ 869, 47